

Effect of Solubilization of Aliphatic Hydrocarbons on Size and Shape of Rodlike C₁₆TABr Micelles Studied by ²H NMR Relaxation

Maria Törnblom* and Ulf Henriksson

Division of Physical Chemistry, Royal Institute of Technology, S-100 44 Stockholm, Sweden

Received: March 11, 1997; In Final Form: May 30, 1997[⊗]

Multifield ²H relaxation has been used to quantify the effect of solubilization of alkanes on the size and shape of the micelles in aqueous solutions of hexadecyltrimethylammonium bromide, C₁₆TABr. Information about aggregate size and shape was deduced from the reorientation rate of the aggregates. The surfactant concentration was chosen so that the solutions without solubilizate contained moderately long rodlike micelles (axial ratio ~4). It was found that the change in aggregation behavior upon solubilization is substantially different for solubilizates of similar chemical composition but different structures. Solubilization of small amounts of cyclohexane, cyclooctane, cyclodecane, *trans*-decalin, *n*-hexane, 2,3-dimethylbutane, or adamantane causes growth of the micelles. Further addition of these solubilizates (except for adamantane, which has a lower solubility limit than the other solubilizates) causes a decrease in the aggregate size. On the other hand, solubilization of *n*-octane, *n*-decane, or *n*-dodecane causes a decrease in aggregate size even in small amounts. It was also found that when the rodlike micelles grow due to the presence of solubilizate molecules, they grow in the axial direction at a constant radius, while the decrease in size at higher solubilizate content occurs as a shortening of the rods accompanied by an increase in radius. The differences in effects are explained by different solubilization sites *within* the micelle for alkanes with different molecular volume and rigidity.

Introduction

When hydrophobic molecules are dissolved in an aqueous micellar solution of a surfactant, they predominantly dissolve in the surfactant aggregates, a process called solubilization.^{1–3} In this process the solubilizate molecules shift the delicate balance of intermolecular forces, determining equilibrium properties such as the average shape and aggregation number of the aggregates in the solution. These effects are well-known, and they have been investigated in a number of studies employing different experimental techniques.

The results of most of the studies on solubilization and aggregation behavior have common features, and together they paint a fairly consistent picture of the phenomenon. Polar substances, most often alcohols and amines, dissolve with their polar groups at the hydrocarbon/water interface of the micelle. Hence they decrease the surface charge density of ionic micelles and thereby promote the formation of micellar geometries with lower mean curvature like rods and, in some systems, discs.^{4–11} They also decrease the degree of counterion binding.⁴ Aromatic hydrocarbons have effects similar to those of alcohols in solutions of cationic surfactants, where they are believed to interact specifically with the positively charged headgroups and thus dissolve at the micellar surface, at least in the initial stages of addition.^{4–7,12–21} Aliphatic hydrocarbons (and aromatic hydrocarbons solubilized in anionic micelles) have quite the opposite effects. Due to their higher hydrophobicity, they are believed to dissolve in the hydrocarbon core part of the aggregates. They increase the aggregate radius when solubilized in spherical micelles and cause transition of rodlike micelles to globular.^{5–9,13,19} Furthermore, the transition of globular to rodlike micelles upon the addition of alcohols is suppressed by the presence of aliphatic hydrocarbons,¹⁶ whereas they have little effect on surface charge density^{4,21} and, in contrast to alcohols, slow down micellar kinetics.¹²

An aliphatic hydrocarbon inducing growth of rodlike micelles does not fit into this picture. Such behavior has been observed

though. Klason²² found that addition of cyclohexane increases the average size of the rodlike micelles in 0.37 mol·kg^{−1} C₁₆-TABr solutions. The growth-inducing effect of cyclohexane has also been demonstrated by Hoffman and co-workers in studies of solubilization in viscoelastic solutions of cationic surfactant/NaSal(alcohol). These authors also found that shorter *n*-alkanes (up to C₈ or C₁₀ depending on the surfactant) cause growth of the extremely long micelles in these solutions when small amounts are added.^{5,6,14,15} Lindemuth and Bertrand¹⁶ have studied the sphere-to-rod transition upon solubilization of pentanol. They found that the presence of cyclohexane promotes the transition in C₁₄TABr/NaBr but not in SDS/NaCl solutions. There have also been reports of alkanes inducing micellar growth in systems where the micelles are disclike. Lianos *et al.* have studied the solubilization of alkanes in mixed SDS/1-pentanol micelles and observed that the aggregation number increases, remains constant, or decreases depending on the chain length and structure of the alkane.^{7,23,24}

In the work presented here we have employed ²H NMR relaxation to study the effect of solubilization of different alkanes on the size and shape of moderately long rodlike micelles with special emphasis on the effects of cyclohexane. We have chosen to work with the 0.37 mol·kg^{−1} C₁₆TABr solution studied by Klason.²² This system is interesting because the micelles in the neat solution are not extremely large. We have, in an earlier study, found them to be rodlike, with an average aggregation number of 200–250 and average axial ratio of ~4.²⁵ We have initially compared the effects of adding small to moderate amounts of 10 alkanes of different molecular size and rigidity on the ²H spin–lattice, *T*₁, and spin–spin, *T*₂, relaxation times of the selectively deuterated surfactant at 30.7 MHz. The effect of adding a fixed volume fraction of cyclohexane to solutions with different surfactant concentrations was also studied.

The efficiency of the quadrupolar relaxation mechanism and the direct dependence of quadrupolar *T*₂ on the rates of the slowest dynamic processes in the investigated systems make it a sensitive qualitative measure of micellar size, even if measured

[⊗] Abstract published in *Advance ACS Abstracts*, July 15, 1997.

only at a single frequency. These measurements make it possible to see trends and compare the effects of different solubilizates. To further evaluate, and quantify, the effects on the size and shape of the micelles, the field dependence of the relaxation rates has to be measured. In a previous study we used field-dependent ²H spin relaxation to investigate the micellar size and shape in aqueous C₁₆TABr and SDS solutions at various surfactant and electrolyte concentrations.²⁵ The use of the theoretical results of Halle²⁶ and of simple models for the molecular motions and the polydispersity of the aggregates made it possible to obtain average aggregation numbers and micellar shapes. In this study we have applied the method to quantitatively investigate the transition of shape and size of C₁₆-TABr micelles upon addition of four alkanes with different structures and molecular volumes: *n*-hexane, cyclohexane, adamantane, and *n*-dodecane.

Experimental Section

Hexadecyltrimethylammonium bromide- α -*d*₂ was synthesized as described in an earlier paper.²⁵ *n*-Hexane (Merck p.a.), *n*-octane (Fluka puriss.), *n*-decane (Aldrich 99+), *n*-dodecane (Merck p.a.), 2,3-dimethylbutane (Aldrich 99+), cyclohexane (Merck p.a.), cyclooctane (Merck zur Synthese), cyclodecane (Aldrich), and *trans*-decalin (EGA-Chemie 97%) were used as received. Adamantane (Aldrich 99+) was recrystallized in ethanol and dried in vacuum.

Samples were prepared from stock solutions of C₁₆TABr in purified water by weighing the surfactant solution into NMR tubes, whereafter the solubilizates were added by microliter syringe and the tubes flame sealed. The samples containing adamantane were prepared by mixing weighed portions of a solution saturated with adamantane with the neat C₁₆TABr solution. The Adamantane content in the saturated solution was determined with ¹³C NMR on a Bruker AMX 400. In the tables and figures the solubilize contents in the samples are reported as volume fractions of solubilize in the hydrocarbon cores of the micelles, neglecting solubility in the intermicellar aqueous solution. The volume of a C₁₆ alkyl chain was taken as 457.8 Å³.²⁷

²H NMR measurements were performed with a Bruker MSL 200/90 spectrometer equipped with a 4.7 T cryomagnet (at 30.7 MHz) or a variable-field iron core magnet (at 2–13.8 MHz) and with a Bruker AM 400 spectrometer (at 61.4 MHz). *T*₁ was determined with the standard inversion recovery method. *T*₂ was determined at 30.7 MHz with the CPMG method where only every second echo was used and the intensities were fitted to an exponentially decreasing function with a constant to account for naturally occurring HDO. Measurements were performed at 30 °C with an estimated uncertainty of ±0.5 °C. The experimental uncertainties in the relaxation rates arise mainly from this variation in temperature. The magnitudes of the uncertainties are difficult to assess (this is why no error bars are given for the experimental points), but it can be assumed that they are larger in *R*₂ than in *R*₁ and larger at lower fields. The errors are also larger for the samples where the aggregation number is high and very sensitive to temperature. The figures showing experimental data (Figures 6 and 7) give an impression of the variations. The deviations of the *R*₂ points from the uppermost curve in Figure 6 represent the maximal variation encountered in these measurements.

Results of Single-Field Measurements

The ²H longitudinal relaxation rate *R*₁ = *T*₁^{−1} measured at a rather high frequency mainly reflects the local motions of the α -segment in the alkyl chain, while the slower motions of the whole micelle are reflected in the transverse relaxation rate *R*₂ = *T*₂^{−1}.²⁵ Increased micellar size and consequently slower

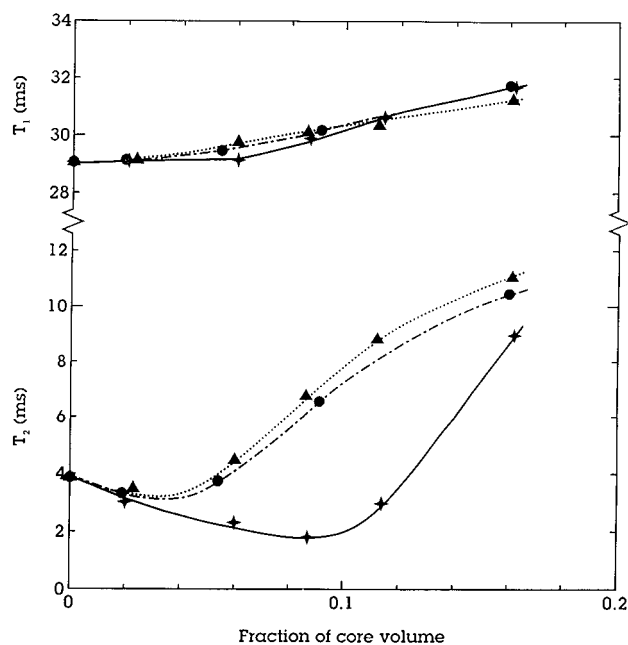


Figure 1. ²H relaxation times at 30.7 MHz and 30 °C for 0.37 mol·kg^{−1} C₁₆TABr with three C₆ alkanes: *n*-hexane (●), 2,3-dimethylbutane (▲), and cyclohexane (★).

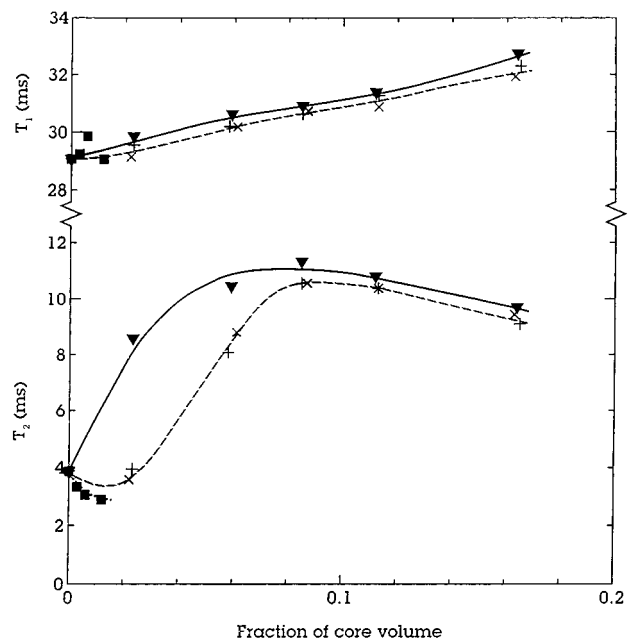


Figure 2. ²H relaxation times at 30.7 MHz and 30 °C for 0.37 mol·kg^{−1} C₁₆TABr with four C₁₀ alkanes: *n*-decane (▼), cyclodecane (×), *trans*-decalin (+), and adamantane (■).

reorientation rate therefore give rise to an increase in the observed *R*₂ values, and qualitative information can be obtained from relaxation rates measured at one high frequency.

The results of such measurements are presented in Figures 1–4. The variation of the *T*₂ shows that aliphatic hydrocarbons can cause either an increase or a decrease in the average size of rodlike C₁₆TABr micelles depending on the molecular structure and the added amount of the solubilize. All solubilizates studied have small effects on the *T*₁ values, indicating only minor effects on the local mobility of the α -methylene segment. This is an indication that the variations in *T*₂ reflect changes of micellar size rather than changes in the order parameter.

To study the effect of molecular structure, three C₆ and four C₁₀ alkanes were investigated (Figures 1 and 2). Most of these cause an initial increase in the micellar size upon solubilization.

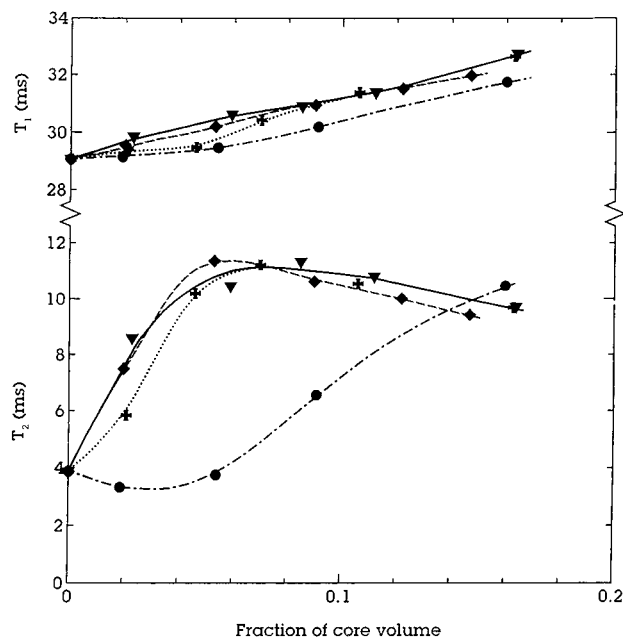


Figure 3. ^2H relaxation times at 30.7 MHz and 30 °C for $0.37 \text{ mol}\cdot\text{kg}^{-1}$ C_{16}TABr with four straight-chain alkanes: *n*-hexane (●), *n*-octane (+), *n*-decane (▼), and *n*-dodecane (◆).

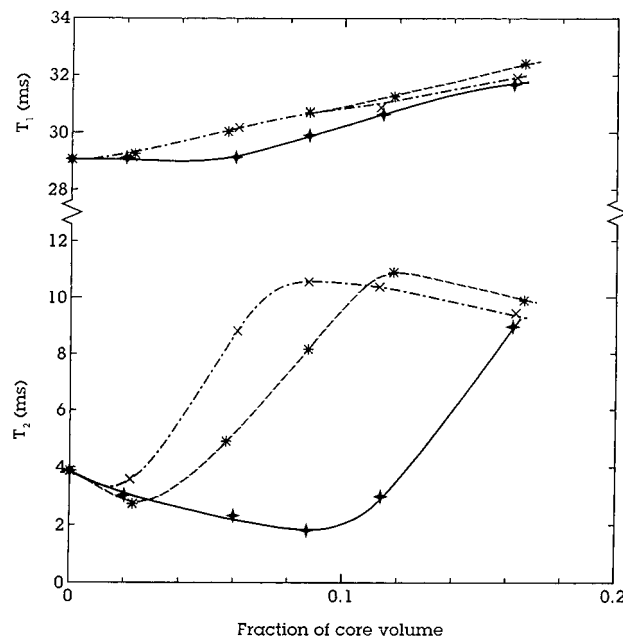


Figure 4. ^2H relaxation times at 30.7 MHz and 30 °C for $0.37 \text{ mol}\cdot\text{kg}^{-1}$ C_{16}TABr with three cycloalkanes: cyclohexane (★), cyclooctane (*), and cyclodecane (×).

The effect is more pronounced for the smaller and more rigid solubilize molecules and largest for cyclohexane, which at most causes a shortening of T_2 from 4 to 2 ms. The very rigid and almost spherical adamantane also seems to have a large effect but has a very low solubility limit. For *n*-hexane and 2,3-dimethylbutane the effect is much smaller, and for the mono- and bicyclic decanes it is merely hinted at at very low volume fractions. Solubilization of *n*-decane, on the other hand, reduces the micellar size considerably already at low solubilize content.

The effect of molecular size was investigated further by comparison of solubilizes with similar structures but different sizes (Figures 3 and 4). Both with the straight chain and the cyclic alkanes there are significant differences in effects on going from six to eight to ten carbons. For the cyclic compounds these differences are probably a result not only of increasing size but also of the increasing flexibility of the cyclic backbone.

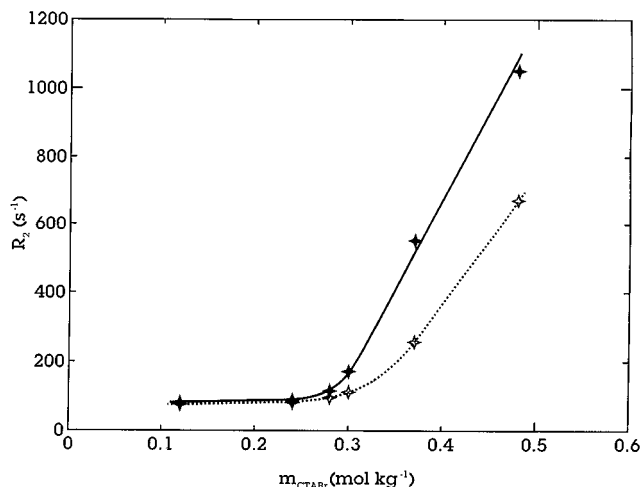


Figure 5. ^2H spin-spin relaxation rates at 30.7 MHz and 30 °C as a function of surfactant concentration for C_{16}TABr solutions without solubilize (empty symbols, ...) and with cyclohexane added in an amount corresponding to 9% of the surfactant chain volume (filled symbols, —).

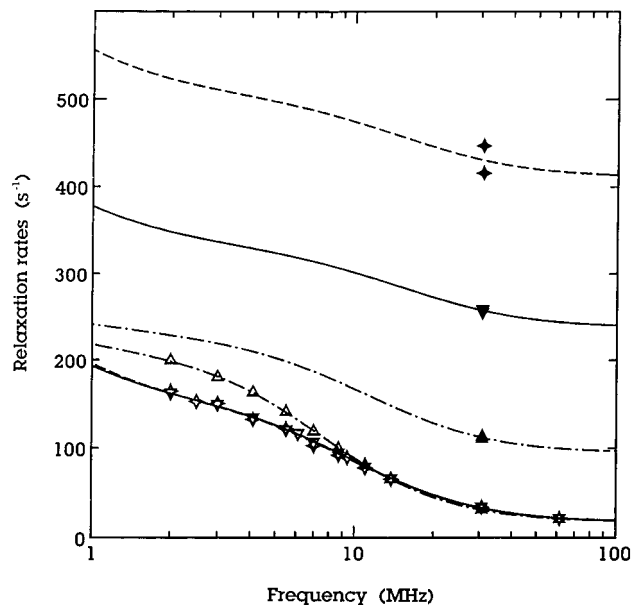


Figure 6. Frequency dependence of ^2H R_1 (empty symbols) and R_2 (filled symbols) at 30 °C for $0.37 \text{ mol}\cdot\text{kg}^{-1}$ C_{16}TABr samples without solubilize (▽, ▼, —) and with cyclohexane at two concentrations: 6% by core volume (☆, ★, - -) and 16% by core volume (△, ▲, ···). The lines represent four-parameter fittings of exponentially distributed spherocylinders.

The effect of cyclohexane solubilization in solutions with different C_{16}TABr concentrations was also studied (Figure 5). It is seen that solubilization of 9% cyclohexane by volume in the hydrocarbon core causes an increase in the micellar size only for surfactant concentrations above the so-called second cmc, the concentration above which rodlike micelles appear in considerable amounts.

In order to extract detailed quantitative information, it is necessary to have experimental data in a wide frequency range.^{25,28–32} To this end we have performed variable-frequency measurements of the ^2H spin-lattice relaxation rate R_1 in the range 2–61.4 MHz for the solutions containing solubilized cyclohexane, *n*-hexane, *n*-dodecane, or adamantane in $0.37 \text{ mol}\cdot\text{kg}^{-1}$ C_{16}TABr and cyclohexane in $0.18 \text{ mol}\cdot\text{kg}^{-1}$ C_{16}TABr . Figures 6 and 7 show some typical results. These data are analyzed quantitatively as described in the next section.

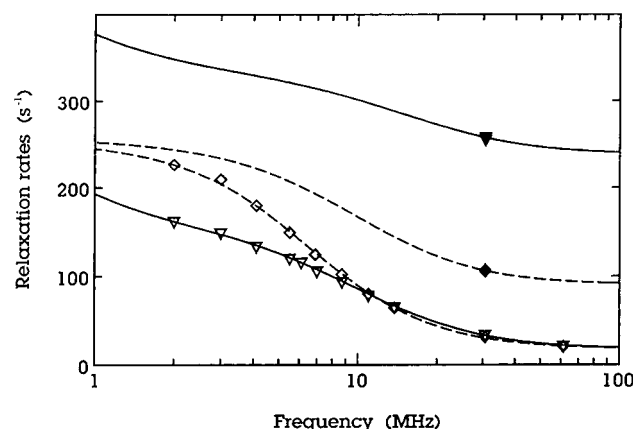


Figure 7. Frequency dependence of ^2H R_1 (empty symbols) and R_2 (filled symbols) at 30 °C for 0.37 mol·kg⁻¹ C₁₆TABr samples without solubilize ($\nabla, \blacktriangledown, -$) and with *n*-dodecane (15% by core volume) ($\diamond, \blacklozenge, - -$). The lines represent four-parameter fittings of exponentially distributed spherocylinders.

Quantitative Evaluation of the Field-Dependent Relaxation Data

Theoretical Background. The fundamental principle behind the investigation of aggregation behavior by the measurement of spin relaxation rates is their dependence on the dynamics of molecular reorientation as expressed by the spectral density function $J(\omega)$, the Fourier transform of the autocorrelation function $g(\tau)$ of the fluctuations of the second-rank interactions. For a quadrupole nucleus, like ^2H , in a position with the quadrupole coupling constant χ in an isotropic system the relaxation rates at Larmor frequency ω_0 are³³

$$R_1(\omega_0) = T_1^{-1}(\omega_0) = \frac{3\pi^2}{20} \chi^2 [2J(\omega_0) + 8J(2\omega_0)] \quad (1)$$

$$R_2(\omega_0) = T_2^{-1}(\omega_0) = \frac{3\pi^2}{20} \chi^2 [3J(0) + 5J(\omega_0) + 2J(2\omega_0)] \quad (2)$$

Through this dependence the field dependence of the relaxation rates may be interpreted quantitatively, in terms of shapes and sizes of micellar aggregates, if models for the molecular motions are provided. The dynamic models that we employ in our work and the derivation of the connected autocorrelation functions, based on the work by Halle,²⁶ have been discussed thoroughly in an earlier paper,²⁵ and we only give the final equations here.

Molecular motions in micellar systems can be categorized into two types occurring on different time scales.^{28,29,31} The spectral density function then separates into two terms,³⁴ where the term for the fast motions, with correlation times corresponding to frequencies outside the NMR range, usually is approximated as a single Lorentzian with correlation time τ^f .

$$J(\omega) = S_{\text{loc}}^2 J^s(\omega) + (1 - S_{\text{loc}}^2) \frac{\tau^f}{1 + (\omega\tau^f)^2} \quad (3)$$

The second-rank local order parameter, S_{loc} , reflects the residual coupling not averaged by the fast motion and is thus a measure of the confinement of the ^2H -labeled methylene.

The slow part of the spectral density, $J^s(\omega)$, describes the final averaging of the second-rank interaction through slower processes. In the present model we consider only the rotational diffusion of the entire micellar aggregates and the lateral diffusion of the surfactant molecules over the curved surfaces of aggregates.²⁵ Halle has shown that the mixed autocorrelation function for simultaneous rotation and lateral diffusion is a sum of four terms.²⁶ Generally only one is a single exponential,

but if the contributions from the lateral diffusion are approximated to have exponential form, then all four terms are exponential and in the slow spectral density become Lorentzians:

$$J^s(\omega) = S_{\text{agg}}^2 \frac{\tau_0^{\text{rot}}}{1 + (\omega\tau_0^{\text{rot}})^2} + \sum_{m=0}^2 (2 - \delta_{m0}) g_m^{\text{diff}}(0) \frac{\tau_m}{1 + (\omega\tau_m)^2} \quad (4)$$

The weight factors in this expression, the aggregate order parameter, S_{agg} , and the $g_m^{\text{diff}}(0)$, are exact despite of the approximations, and they are all simple averages of trigonometric functions over the surface. The joint correlation times are given by

$$\frac{1}{\tau_m} = \frac{1}{\tau_m^{\text{rot}}} + \frac{1}{\tau_m^{\text{diff}}} \quad (5)$$

The rotational diffusion coefficients required to calculate the rotation correlation times,³⁵ τ_m^{rot} , are available for both spheroids³⁶ and cylinders with hemispherical endcaps.³⁷ In a further approximation, the "initial slope approximation",²⁶ the diffusion correlation times, τ_m^{diff} , can be obtained as simple expressions of aggregate dimensions and the coefficient of lateral diffusion over the aggregate surface, D_{lat} .²⁵ For a spherical micelle $S_{\text{agg}} = 0$ and the τ_m are independent of the index. As a consequence, $J^s(\omega)$ reduces to a single term and the full spectral density, eq 3, to a Lorentzian two-step function.

Fittings of Motional Models to Experimental Data. The spectral density function (4) applies to the molecules in an aggregate of specific shape and size. Micellar solutions are polydisperse, however, and it is more correct to include polydispersity in the model for the evaluation of relaxation measurements. Such a model was also found to provide a better description of data from the C₁₆TABr/water and SDS/NaCl/water systems.²⁵ The measurable spectral density for a polydisperse micellar solution, where the molecular exchange is fast compared to the relaxation rates, is an average over the spectral densities of the molecules in the different aggregates. In three-component systems such as those we are treating here, there is polydispersity in the number of solubilize molecules, m , as well as in the number of surfactant molecules, n , per micelle, and micelles with the same aggregation numbers may also take on different shapes. The real distribution function of n and m is unknown; this is why simplifying assumptions are necessary. Assuming that the distribution in m is narrow and centered around the stoichiometric amount for every n , we may treat the solubilize/surfactant ratio, x , as constant for all aggregates in the distribution and the m -dependence is dropped. If we further assume that the aggregation number n specifies the shape of an aggregate, that the fast motion is independent of the shape and size of the aggregate, and that the contribution from the surfactant monomers in the intermicellar solution can be neglected, we get

$$J(\omega) = (1 - S_{\text{loc}}^2) \frac{2\tau^f}{1 + (\omega\tau^f)^2} + S_{\text{loc}}^2 \int_{n_{\text{min}}}^{\infty} f(n) J^s(n, \omega) dn \quad (6)$$

where the hydrocarbon core volume needed for the calculation of $J^s(n, \omega)$ is taken as that of n surfactant chains and nx solubilized molecules together. In our work on the C₁₆TABr/water and SDS/NaCl/water systems we found that the simplest model of the polydispersity, an exponentially decreasing distribution of aggregation numbers starting with spheres,

TABLE 1: Parameter Values from Fittings of the Exponential Distribution of Spherocylinders Described in the Text to Experimental Data from Samples with 0.37 mol·kg⁻¹ C₁₆TABr^a

solubilizate	φ_{sol}	$\langle n_{\text{CTABr}} \rangle^{b,c}$	$\langle n_{\text{sph}} \rangle^{b,c}$	R_{sph}^b (Å)	S_{loc}^b	τ^{fb} (ps)	rms dev (%)
	0	223 ⁺¹³ ₋₀₉	0	25.0 ^{+0.5} _{-0.3}	0.185 ^{+0.002} _{-0.002}	38 ⁺¹ ₋₁	1.2
<i>n</i> -C ₆ H ₁₄	0.02	233 ⁺¹⁶ ₋₁₄	10 ⁺¹ ₋₁	25.2 ^{+0.5} _{-0.5}	0.185 ^{+0.003} _{-0.002}	38 ⁺¹ ₋₂	1.6
<i>n</i> -C ₆ H ₁₄	0.05	213 ⁺¹⁹ ₋₁₆	26 ⁺² ₋₂	25.1 ^{+0.7} _{-0.7}	0.184 ^{+0.004} _{-0.003}	37 ⁺² ₋₃	2.2
<i>n</i> -C ₆ H ₁₄	0.09	180 ⁺¹⁰ ₋₁₁	38 ⁺² ₋₂	26.1 ^{+0.5} _{-0.5}	0.184 ^{+0.003} _{-0.002}	36 ⁺² ₋₂	1.8
<i>n</i> -C ₆ H ₁₄	0.16	162 ⁺⁶ ₋₆	65 ⁺³ ₋₂	29.2 ^{+0.5} _{-0.4}	0.184 ^{+0.001} _{-0.002}	36 ⁺¹ ₋₂	1.2
C ₆ H ₁₂	0.02	237 ⁺¹⁶ ₋₁₀	12 ⁺¹ ₋₁	24.9 ^{+0.6} _{-0.4}	0.186 ^{+0.002} _{-0.003}	38 ⁺² ₋₂	1.8
C ₆ H ₁₂	0.06	250 ⁺²⁶ ₋₁₈	41 ⁺⁴ ₋₃	24.9 ^{+0.8} _{-0.6}	0.185 ^{+0.003} _{-0.004}	38 ⁺² ₋₂	2.3
C ₆ H ₁₂	0.09	268 ⁺²⁰ ₋₁₄	65 ⁺⁵ ₋₃	25.1 ^{+0.6} _{-0.4}	0.187 ^{+0.002} _{-0.003}	37 ⁺² ₋₁	1.7
C ₆ H ₁₂	0.11	248 ⁺¹⁴ ₋₁₃	81 ⁺⁴ ₋₄	26.3 ^{+0.5} _{-0.5}	0.186 ^{+0.002} _{-0.002}	37 ⁺¹ ₋₂	1.6
C ₆ H ₁₂	0.16	191 ⁺⁰⁵ ₋₀₅	94 ⁺³ ₋₃	29.2 ^{+0.3} _{-0.3}	0.184 ^{+0.001} _{-0.001}	38 ⁺¹ ₋₁	1.0
C ₁₀ H ₁₄	0.003	233 ⁺¹⁸ ₋₁₇	2 ⁺⁰ ₋₀	25.0 ^{+0.6} _{-0.7}	0.187 ^{+0.004} _{-0.003}	38 ⁺¹ ₋₃	1.9
C ₁₀ H ₁₄	0.006	242 ⁺²⁴ ₋₂₄	3 ⁺⁰ ₋₀	25.0 ^{+0.8} _{-0.8}	0.186 ^{+0.005} _{-0.004}	38 ⁺² ₋₃	2.3
C ₁₀ H ₁₄	0.01	238 ⁺¹⁹ ₋₁₉	6 ⁺¹ ₋₁	24.8 ^{+0.6} _{-0.7}	0.187 ^{+0.004} _{-0.003}	38 ⁺² ₋₃	1.9
<i>n</i> -C ₁₂ H ₂₆	0.02	188 ⁺¹⁰ ₋₁₀	5 ⁺⁰ ₋₀	26.2 ^{+0.4} _{-0.5}	0.183 ^{+0.002} _{-0.002}	37 ⁺¹ ₋₂	1.5
<i>n</i> -C ₁₂ H ₂₆	0.05	164 ⁺⁰⁹ ₋₀₈	11 ⁺¹ ₋₁	28.3 ^{+0.7} _{-0.6}	0.181 ^{+0.002} _{-0.002}	37 ⁺¹ ₋₂	1.6
<i>n</i> -C ₁₂ H ₂₆	0.09	185 ⁺⁰⁹ ₋₀₉	22 ⁺¹ ₋₁	29.9 ^{+0.8} _{-0.6}	0.183 ^{+0.002} _{-0.002}	38 ⁺¹ ₋₂	1.7
<i>n</i> -C ₁₂ H ₂₆	0.12	203 ⁺⁰⁹ ₋₁₀	34 ⁺² ₋₂	31.0 ^{+0.8} _{-0.7}	0.184 ^{+0.002} _{-0.002}	38 ⁺¹ ₋₂	1.8
<i>n</i> -C ₁₂ H ₂₆	0.15	217 ⁺¹² ₋₁₀	45 ⁺² ₋₂	31.8 ^{+1.0} _{-0.5}	0.186 ^{+0.003} _{-0.002}	39 ⁺² ₋₂	2.0

^a The lateral diffusion coefficient was held at $76 \times 10^{-12} \text{ m}^2 \cdot \text{s}^{-1}$ for C₁₆TA⁺. The ratios of the radius of very long aggregates to that of spherical aggregates were held constant at 0.75. ^b The error limits represent 90% confidence intervals and were determined with Monte Carlo calculations (100 repetitions). ^c The aggregation numbers were calculated from the hydrocarbon core volume assuming a headgroup length of 4.0 and a chain volume of 457.8 Å³ for the hexadecyl group. The volumes of the solubilizate molecules were taken as those of the pure substances.

$$f(n) = \frac{1}{\langle n \rangle - n_{\text{sph}}} e^{-(n - n_{\text{sph}})/(\langle n \rangle - n_{\text{sph}})} \quad (7)$$

gave an excellent description of the experimental relaxation data provided that a gradual decrease in the micellar radius, from R_{sph} for a spherical micelle with aggregation number n_{sph} to R_{∞} for an infinitely long micelle in the same distribution, was introduced.²⁵ In eq 7 $\langle n \rangle$ denotes the number of surfactant molecules in a weight average micelle. With the assumptions stated earlier, this model (eqs 6 and 7) can readily be applied to micelles containing solubilized molecules.

In our previous work the core radius of the spherical micelle was assumed to be that of the extended surfactant chain and R_{∞} was varied in the fitting procedure. This is not a suitable procedure for three-component systems where the radius can exceed the maximal length of the alkyl chain. The ratio of these two radii may, however, be kept constant to $R_{\infty} = 0.75R_{\text{sph}}$, as found to be within error limits for most investigated samples in the C₁₆TABr/water system.²⁵ R_{sph} may then be varied in the fittings. This makes it possible to evaluate the relaxation data from the C₁₆TABr/water/alkane systems using only four adjustable parameters: (i) the radius R_{sph} of the spherical micelles in the distribution; (ii) the width of the distribution, which is related to the aggregation number of a weight average micelle, $\langle n \rangle$; (iii) the local order parameter, S_{loc} ; and (iv) the correlation time for the fast molecular motions, τ^f .

The field-dependent relaxation data (²H R_1 in the range 2–61.4 MHz and R_2 at 30.7 MHz) were analyzed by simultaneous fittings of eqs 1 and 2 with eqs 3–7 using the Unifit program.³⁸ The aggregates were treated as spherocylinders (cylindrical rods with hemispherical endcaps) in the “initial slope approximation”.^{25,26} The τ_m^{rot} that appear in eqs 4 and 5 depend on the geometrical dimensions of the aggregate via the rotational diffusion coefficients for which Yamakawa’s and Yoshizaki’s

results were used.³⁷ The effect of neighboring aggregates on the rotational diffusion was taken care of by a correction factor in the viscosity of the water according to Montgomery and Bernes hard sphere model.³⁹ The $g_m^{\text{diff}}(0)$ depend only on the geometry of the aggregates, while the τ_m^{diff} also depend on the lateral diffusion coefficient of the surfactant cation which, in all fittings, was held constant to $D_{\text{lat}} = 76 \times 10^{-12} \text{ m}^2 \cdot \text{s}^{-1}$ as in our previous work.²⁵ The quadrupole coupling constant was set to $\chi = 181 \text{ kHz}$.^{30,40}

The single-exponential model fit all data sets within 3% rms deviation, in fact most of them within 2%. Results for some representative samples are shown in Figures 6 and 7. Since this simple model is sufficient to describe experimental data, it is not meaningful to introduce a more complicated distribution function. Neither is it, in our opinion, meaningful to change the distribution function of eq 7 because of the presence of solubilizate, even though this may be theoretically correct.⁴¹ The true distribution is still unknown, and eq 7 may be as good an approximation as any, especially since the functional form of the distribution has no major effect on the fitting results.

Apart from the exponential distribution model monodisperse models with spheroidal (prolate or oblate) aggregate shapes were also tested. The pattern in these fittings very much resembles that found for the C₁₆TABr/water system at different concentrations.²⁵

Results

The parameter values for the best fittings of the exponentially distributed spherocylinders model to the experimental relaxation rates are presented in Table 1. The aggregation number, axial ratio, and radius of a weight average micelle as functions of the solubilizate volume fraction are presented in Figure 8.

These results show that the growth in micellar size, indicated qualitatively by the single-field data presented above, is indeed an elongation of the average micelle. In the cyclohexane and adamantane systems this initial elongation is significant, while the elongation caused by the addition of very small amounts of *n*-hexane is small. A very interesting feature is that the initial growth occurs *only* in the axial direction. There is no indication of radial growth of the micelles until they reach their maximal length. Further addition of solubilizate causes a considerable shortening of the micelles, which is accompanied by a simultaneous increase in radius. For *n*-dodecane there is no initial elongation, and the shortening/radial growth effect is even more pronounced. We also see that the radial growth continues after globular form is reached.

One might find these results to be a rather uncertain since the evaluation of the data is both model dependent and based on a number of assumptions. The effects are, however, clearly visible in the raw relaxation data presented in Figures 6 and 7. For rodlike micelles the dispersion in R_1 is dominated by the contributions from the reorientation around the long axis of the micelle, and R_1 thus mainly depends on the radius while R_2 , which in addition depends on $J(0)$, contains more information about the length of the rods. Figure 6 shows that the R_1 data from the neat 0.37 mol·kg⁻¹ C₁₆TABr solution and the solution with $\varphi = 0.06$ cyclohexane fall on the same curve despite that R_2 for the sample containing cyclohexane is significantly higher. The data for the sample with $\varphi = 0.15$ cyclohexane are also included in the figure. For this solution R_2 is lower, but the inflection point of the R_1 curve is shifted to lower frequencies, an indication of radial growth. This effect is even stronger in the data of Figure 7, which compares a sample containing *n*-dodecane with $\varphi = 0.15$ to the neat C₁₆TABr solution. The frequency shift in the R_1 dispersion could reflect a change in D_{lat} instead of radial growth, but for this to be the sole

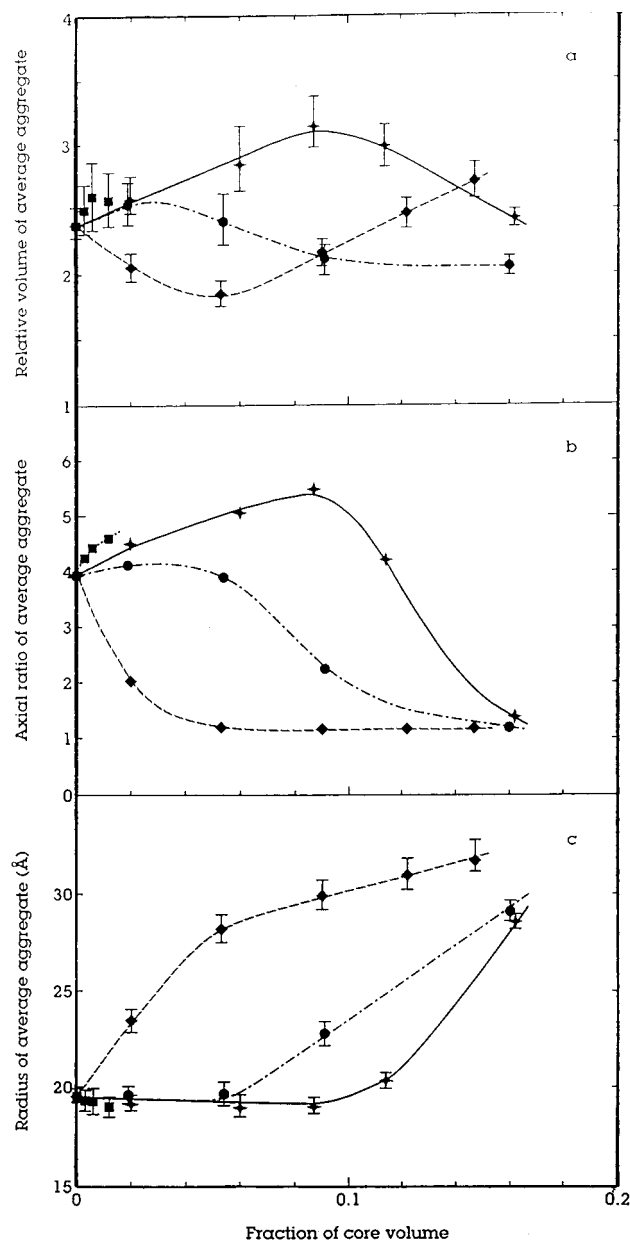


Figure 8. Size and shape parameters from the fitting results for 0.37 mol·kg⁻¹ C₁₆TABr with *n*-hexane (●), cyclohexane (★), adamantane (■), or *n*-dodecane (◆). (a) Hydrocarbon core volume of a weight average aggregate relative to that of a spherical micelle with the core radius equal to the length of an all-*trans* C₁₆-chain. (b) Axial ratio of a weight average aggregate (the error limits are contained in the symbols). (c) Radius (or short axis) of a weight average aggregate (including headgroup).

explanation D_{lat} would have to decrease to one-fourth of its original value with the addition of 15% *n*-dodecane. A substantial decrease in D_{lat} could only be brought about by changes in molecular organization that would be reflected in changes in S_{loc} and τ^f . These parameters are, however, practically constant throughout the investigated range of volume fractions for all the solubilizates studied. This constancy is in itself a noteworthy result of this investigation.

To verify the conclusions of the data in Figure 5 and quantify the effect of the solubilization of cyclohexane in solutions below the second cmc (*vide supra*), the field dependence of the relaxation rates was measured for three samples with 0.18 mol·kg⁻¹ C₁₆TABr. The results from the analysis are presented in Table 2. Solubilization of cyclohexane in these small micelles does not lead to the formation of longer rodlike micelles. At low solubilizate content there is no significant change in micellar size, and near the solubility limit we see radial growth but no

TABLE 2: Parameter Values from Fittings of the Exponential Distribution of Spherocylinders Described in the Text to Experimental Data from Samples with 0.18 mol·kg⁻¹ C₁₆TABr and Cyclohexane^a

φ_{sol}	$\langle n_{CTABr} \rangle^{b,c}$	$\langle n_{sol} \rangle^{b,c}$	R_{sph}^b (Å)	S_{loc}^b	τ^f (ps)	rms dev (%)
0	139 ⁺¹¹ ₋₁₀	0	26.8 ^{+0.9} _{-0.8}	0.177 ^{+0.004} _{-0.004}	37 ⁺² ₋₂	2.1
0.06	115 ⁺⁷ ₋₆	19 ⁺¹ ₋₃	25.6 ^{+0.6} _{-0.5}	0.177 ^{+0.003} _{-0.003}	36 ⁺¹ ₋₂	1.5
0.21	166 ⁺⁶ ₋₆	90 ⁺³ ₋₃	29.8 ^{+0.8} _{-0.6}	0.178 ^{+0.002} _{-0.001}	38 ⁺¹ ₋₁	1.2

^a The lateral diffusion coefficient was held at 76×10^{-12} m²·s⁻¹ for C₁₆TA⁺. The ratios of the radius of very long aggregates to that of spherical aggregates were held constant at 0.75 (see ref 25). ^b The error limits represent 90% confidence intervals and were determined with Monte Carlo calculations (100 repetitions). ^c The aggregation numbers were calculated from the hydrocarbon core volume assuming a headgroup diameter of 4.0 and a chain volume of 457.8 Å³ for C₁₆TA⁺. The volumes of the solubilizate molecules were taken as those in the pure substances.

TABLE 3: Parameter Values from Fittings of the Two-Step Model for Those Samples Where the Model Fit within 6% rms Deviation

m_{CTABr} (mol/kg)	solubilizate	φ_{sol}	τ^s (ns)	$R_{sph}^{a,b}$ (Å)	rms dev (%)
0.37	<i>n</i> -C ₆ H ₁₄	0.16	11.4 ^{+0.3} _{-0.3}	31.3 ^{+0.3} _{-0.3}	1.7
0.37	<i>n</i> -C ₁₂ H ₂₆	0.05	10.6 ^{+0.4} _{-0.4}	30.4 ^{+0.4} _{-0.4}	2.0
0.37	<i>n</i> -C ₁₂ H ₂₆	0.09	12.0 ^{+0.3} _{-0.4}	32.0 ^{+0.3} _{-0.4}	2.0
0.37	<i>n</i> -C ₁₂ H ₂₆	0.12	13.2 ^{+0.3} _{-0.4}	33.2 ^{+0.3} _{-0.4}	2.2
0.37	<i>n</i> -C ₁₂ H ₂₆	0.15	14.2 ^{+0.5} _{-0.4}	34.3 ^{+0.5} _{-0.5}	2.5
0.18		0	9.1 ^{+0.3} _{-0.4}	28.6 ^{+0.3} _{-0.5}	2.3
0.18	C ₆ H ₁₂	0.06	9.1 ^{+0.2} _{-0.3}	28.6 ^{+0.3} _{-0.4}	2.0
0.18	C ₆ H ₁₂	0.21	12.0 ^{+0.2} _{-0.3}	31.9 ^{+0.3} _{-0.3}	1.2

^a The error limits represent 90% confidence intervals and were determined with Monte Carlo calculations (100 repetitions). ^b R_{sph} was evaluated from τ^s using the lateral diffusion coefficient 76×10^{-12} m²·s⁻¹ for C₁₆TA⁺.

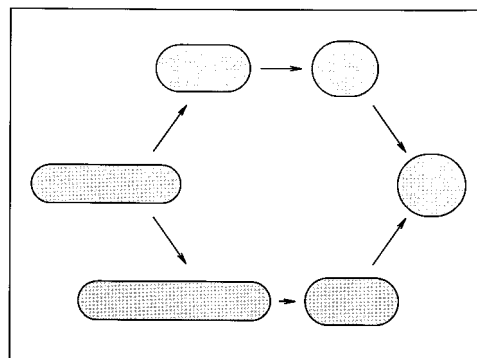


Figure 9. Change in size and shape of rodlike C₁₆TABr micelles with addition of cyclohexane (lower path) and *n*-dodecane (upper path). Of the studied alkanes, these two had the strongest effects on the aggregation behavior.

significant change in axial ratio. Thus, we may conclude that the growth-inducing effect of cyclohexane is a weak one since the existence of rodlike micelles is a prerequisite for it to occur.

For some of the samples yielding low axial ratios in the fittings discussed above the sphere model also fit with good accuracy, and the results of these fittings are presented in Table 3.

The most important features of the results from the fittings are summarized schematically in Figure 9, which, approximately drawn to scale, compares the effects of the addition of two alkanes with different structures and molecular volumes. The long, straight-chain *n*-dodecane causes a monotonous transition to globular micelles with simultaneous radial growth (upper path). This behavior will henceforth be called the "rod-to-sphere transition" despite the lack of experimental evidence of the resulting micelles being perfectly spherical. The small, rigid

cyclohexane initiates axial growth at a constant radius, before the shortening and thickening starts (lower path). The results of the single-field measurements presented earlier (Figures 1–4) indicate that between these two extremes there is a continuous range of effects that depend on the size and structure of the solubilize in a systematic way.

Discussion

Micellar solutions are polydisperse. It is the variation of the standard chemical potential of the surfactant with shape and aggregation number that, in balance with the entropy of dispersion, determines their equilibrium properties, *e.g.* the shape and size of the average micelle. In a two-component surfactant/water system the most important contributions to the variation of the chemical potential arise from^{42–44} (i) the residual hydrocarbon/water contact at the aggregate interface; (ii) the electrostatic repulsion between the charged headgroups; and (iii) the conformational free energy of the surfactant alkyl chains that are packed into the core and may not assume their most favorable configurations.

All these terms depend explicitly on the area per headgroup and/or the curvature of the micellar interface. The addition of a solubilize alters the geometrical conditions for them and may change the physical properties that determine their magnitudes. It adds a free energy contribution from the mixing of solubilize molecules and surfactant chains and shifts the micellar equilibrium toward higher average aggregation numbers since polydispersity in the number of solubilize molecules as well as in the number of surfactant molecules per micelle results in increased entropy of dispersion.⁴¹ Another important effect of the presence of solubilize is that the restriction that the micellar radius cannot exceed the length of a fully extended (all-*trans*) surfactant molecule is lifted. In two-component systems the radius of the equilibrium spherical micelle is close to or on this limit, while the cylindrical parts of rodlike micelles are somewhat thinner.^{42,46}

As mentioned in the Introduction the effects of an additive on aggregation is commonly correlated to its solubilization site. The classic example is the solubilization of benzene in cationic surfactants. Specific interactions between the benzene molecules and the positively charged headgroups cause the molecules to dissolve preferentially at or near the hydrocarbon/water interface, thereby lowering both the electrostatic repulsion between the headgroups and the hydrocarbon/water contact free energy.^{17,18} Because of this, benzene induces growth and formation of rodlike micelles even in solutions where these do not predominate.¹³ When the outer layer is saturated with benzene, further solubilization takes place inside the core with a consequent transition from rodlike to globular aggregates. The possibility of more than one solubilization site may also be the explanation of the extremely high solubility of benzene in, for example, C₁₆TABr.^{13,47}

If we look at the effect of cyclohexane on C₁₆TABr micelles, it resembles that of benzene though much weaker, and it may be tempting to explain it by a similar mechanism. We do not find this to be a likely explanation. Most alkanes, provided they are small enough compared to the surfactant chains, may cause growth of rod- or disclike micelles if the conditions for the formation of these are favorable enough in the neat surfactant solution.^{5,7,14,15,23,24} It is therefore far more likely that cyclohexane exhibits the extreme of an effect shown by all alkanes to a greater or lesser extent than that it is "surface active" in the sense of benzene. When solubilized, cyclohexane generally has an effect more like that of an alkane than that of an aromatic hydrocarbon,^{4,12,16,21,48,49} and though it is slightly more water soluble than *n*-alkanes, it is much less water soluble than

benzene.⁵⁰ The reason behind the differences in effects on aggregation behavior between the investigated alkanes is therefore, in our opinion, to be sought in more subtle differences in interactions that lead to different solubilization sites *within* the hydrocarbon core. Such a difference has been demonstrated by Boden and Jones for cyclohexane and *n*-tetradecane solubilized in lamellar phases.⁵¹

The effects of solubilizes on aggregation equilibria may be qualitatively discussed in terms of their possible influences on the free energy contributions presented above. The rod-to-sphere transition accompanied by increasing radius may be considered to be the normal effect of the solubilization of nonpolar molecules. It is exhibited by all reasonably soluble solubilizes in this study and is the behavior most commonly observed in other studies.^{5–9,12–16,22–24} The experimental results show that this process results in micellar radii larger than the length of the extended surfactant chain, and it is obvious that it must include the formation of a zone of unmixed solubilize in the center of the micelle. It is not surprising that radial growth occurs when the constraint on the radius is lifted. The driving force behind the growth is the gain in hydrocarbon/water contact free energy with the decrease in the surface area/headgroup that follows from an increase in radius. These conclusions are in full agreement with the results of the theoretical calculations of solubilization equilibria by Landgren *et al.*^{52–54} In our experiments we did not, however, find radial growth to quite the extent they predict. For all solubilizes and concentrations we investigated, a good portion of the solubilize (80% to the minimum) is still mixed with the surfactant chains. As for the simultaneous shortening, it is easy to show by simple geometry that if equal amounts of solubilize form unmixed zones in the centers of a spherical and a cylindrical micellar segment, it increases the radius of the spherical segment more. In consequence the free energy of the spherical segment decreases more than that of the cylindrical. Hence there is free energy to be gained by forming spherical micelles out of cylindrical segments, and the average axial ratio will decrease. We conclude from this that simultaneous decrease in axial ratio is, indeed, a natural consequence of radial growth.

In consequence with the argument above we conclude that the initial elongation effect is found when the solubilize molecules mix with the surfactant alkyl chains rather than forming a center zone. It can always be argued that if the free energy of mixing between solubilize and chains is large enough to compete with the net free energy that can be gained from radial growth, no center zone with unmixed solubilize forms. Thus no thickening, and consequently no shortening, occurs. The radius remains at approximately the length of the surfactant molecule, and the dilution of the headgroups as well as the entropy of dispersion (*vide supra*) favors cylindrical micellar segments. From the volume fraction dependence of the aggregation behavior that we see in our experimental results we conclude that there must be saturation of the surfactant chain part of the micellar core, otherwise the elongation would continue throughout the volume fraction interval. This saturation obviously occurs at different volume fractions for different solubilizes, and with addition above this point the solubilize dissolves in the center and the rod-to-sphere transition with radial growth occurs.

It may seem surprising that molecules of substances so similar in macroscopic properties as the different alkanes studied should interact in such different ways with the surfactant hydrocarbon chains. The fact that they do so shows just how delicate the balance of forces that determine micellar equilibria is. It must also be remembered that the interior of micelles, though liquid-like in nature,⁵⁵ does not resemble bulk liquid. It is subjected

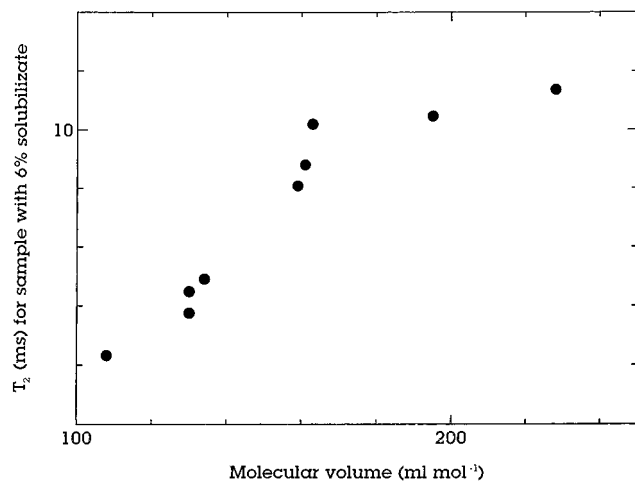


Figure 10. ^2H T_2 at 30.7 MHz from 0.37 mol·kg⁻¹ C₁₆TABr solutions containing ~6% solubilizate by micellar core volume plotted versus the molar volumes of the solubilizates.

to Laplace pressures of several hundred atmospheres⁵⁶ and has nonvanishing order in the outer parts.^{22,28–30,57–59} Under these conditions it is not surprising to find the nonideal mixing behavior necessary to explain the differences. We see in Figures 1–4 that the property that is most important in determining the effect of a solubilizate is molecular size. This is further developed in Figure 10, where the ^2H T_2 at 30.7 MHz of the samples containing ~6% solubilizate are plotted against the molar volume of the solubilizates. Some influence of molecular volume must be expected since a higher number of molecules per unit volume means a higher entropy of mixing at a constant volume fraction, but this is not enough to explain the differences in effects. There must be an additional mechanism, and it is probable that it is of steric origin. We may suspect that a small molecule simply “fits in” a lot easier between the tightly packed hydrocarbon chains and thus is much more efficient in releasing the packing constraints on the chains and lowering their free energy of conformation. The other important factor for the solubilization site is obviously the rigidity of the solubilizate molecule. A probable explanation, suggested by Boden and Jones,⁵¹ is that a long flexible molecule would have to lose conformational entropy to mix with the ordered chains, while a rigid molecule has less conformational entropy to lose and thus mixes more favorably.

In our opinion the results of this study have relevance in the discussions of both solubilization behavior and micellar equilibria in general. In particular they illustrate the importance of the contributions from the conformational state and the intermolecular interactions in the hydrocarbon region of the micelles to the aggregation equilibrium.

Acknowledgment. We want to thank the Swedish Natural Sciences Research Council for financial support, Bertil Halle for making his computer programs available to us, Jan Christer Eriksson and Mikael Börlling for valuable hints and comments, and Ann-Charlotte Hellgren for the synthesis of the deuterium-labeled surfactant.

References and Notes

- (1) *Solubilization in Surfactant Aggregates*; Christian, S. D., Scamehorn, F. F., Eds.; Marcel Dekker: New York, 1995.
- (2) Fendler, J. H.; Fendler, E. J. *Catalysis in Micellar and Macromolecular Systems*; Academic Press: New York, 1975.
- (3) Elworthy, P. H.; Florence, A. T.; Macfarlane, C. B. *Solubilization by Surface-Active Agents*; Chapman and Hall: London, 1968.
- (4) Lindblom, G.; Lindman, B.; Mandell, L. *J. Colloid Interface Sci.* **1973**, *42*, 400.

- (5) Hoffman, H.; Ulbricht, W. *Tenside, Surfactants, Deterg.* **1987**, *24*, 23.
- (6) Bayer, O.; Hoffman, H.; Ulbricht, W.; Thurn, H. *Adv. Colloid Interface Sci.* **1986**, *26*, 177.
- (7) Lianos, P.; Lang, J.; Strazielle, C.; Zana, R. *J. Phys. Chem.* **1982**, *86*, 1019.
- (8) Reekmans, S.; Luo, H.; van der Auweraer, M.; de Schryver, F. C. *Langmuir* **1990**, *6*, 628.
- (9) Zhao, G.-X.; Li, X.-G. *J. Colloid Interface Sci.* **1991**, *144*, 185.
- (10) Durga Prasad, Ch.; Singh, H. N.; Goyal, P. S.; Srinivasa Rao, K. *J. Colloid Interface Sci.* **1993**, *155*, 415.
- (11) Kumar, S.; Aswal, V. K.; Singh, H. N.; Goyal, P. S.; Kabir-ud-Din *Langmuir* **1994**, *10*, 4069.
- (12) Lang, J.; Zana, R. *J. Phys. Chem.* **1986**, *90*, 5258.
- (13) Eriksson, J. C.; Henriksson, U.; Klason, T.; Ödberg, L. In *Solution Behaviour of Surfactants*, Vol. 2; Mittal, K. L., Fendler, E. J., Eds.; Plenum Publishing Corp.: New York, 1982; p 907.
- (14) Bayer, O.; Hoffman, H.; Ulbricht, W. In *Surfactants in Solution*, Vol. 4; Mittal, K. L., Bothorel, P., Eds.; Plenum Publishing Corp.: New York, 1987; p 343.
- (15) Hoffman, H.; Ulbricht, W. *J. Colloid Interface Sci.* **1989**, *129*, 388.
- (16) Lindemuth, P. M.; Bertrand, G. L. *J. Phys. Chem.* **1993**, *97*, 7769.
- (17) Mukerjee, P.; Cardinal, J. R. *J. Phys. Chem.* **1978**, *82*, 1620.
- (18) Eriksson, J. C.; Gillberg, G. *Acta Chem. Scand.* **1966**, *20*, 2019.
- (19) Wasylshen, R. E.; Kwak, J. T. C.; Gao, Z.; Verpoorte, E.; MacDonald, J. B.; Dickson, R. M. *Can. J. Chem.* **1991**, *69*, 822.
- (20) Heindl, A.; Strnad, J.; Kohler, H.-H. *J. Phys. Chem.* **1993**, *97*, 742.
- (21) Valiente, M.; Rodenas, E. *J. Colloid Interface Sci.* **1990**, *138*, 299.
- (22) Klason, T. Thesis, KTH Stockholm, 1982.
- (23) Lianos, P.; Lang, J.; Zana, R. *J. Phys. Chem.* **1982**, *86*, 4809.
- (24) Lianos, P.; Lang, J.; Sturm, J.; Zana, R. *J. Phys. Chem.* **1984**, *88*, 819.
- (25) Törnblom, M.; Henriksson, U.; Ginley, M. *J. Phys. Chem.* **1994**, *98*, 7041. Erratum *J. Phys. Chem.* **1997**, *101*, 3901.
- (26) Halle, B. *J. Chem. Phys.* **1991**, *94*, 3150.
- (27) Tanford, C. *The Hydrophobic Effect*; John Wiley: New York, 1980.
- (28) Söderman, O.; Walderhaug, H.; Henriksson, U.; Stilbs, P. *J. Phys. Chem.* **1985**, *89*, 3693.
- (29) Söderman, O.; Henriksson, U.; Olsson, U. *J. Phys. Chem.* **1987**, *91*, 116.
- (30) Söderman, O.; Henriksson, U. *J. Chem. Soc., Faraday Trans. 1* **1987**, *83*, 1515.
- (31) Ginley, M.; Henriksson, U.; Li, P. *J. Phys. Chem.* **1990**, *94*, 4644.
- (32) Söderman, O.; Carlström, G.; Olsson, U.; Wong, T. C. *J. Chem. Soc., Faraday Trans. 1* **1988**, *84*, 4475.
- (33) Abragam, A. *The Principles of Nuclear Magnetism*; Clarendon: Oxford, 1961; Chapter 8.
- (34) Halle, B.; Wennerström, H. *J. Chem. Phys.* **1981**, *75*, 1928.
- (35) Woessner, D. E. *J. Chem. Phys.* **1962**, *37*, 647.
- (36) Perrin, F. *J. Phys. Radium* **1934**, *5*, 497.
- (37) Yoshizaki, T.; Yamakawa, H. *J. Chem. Phys.* **1980**, *72*, 57.
- (38) Stilbs, P.; Moseley, M. E. *J. Magn. Reson.* **1978**, *31*, 55.
- (39) Montgomery, J. A.; Berne, B. J. *J. Chem. Phys.* **1977**, *67*, 4598.
- (40) Söderman, O. *J. Magn. Reson.* **1986**, *68*, 296.
- (41) Bergström, M.; Eriksson, J. C. *Langmuir* **1991**, *8*, 36.
- (42) Eriksson, J. C.; Ljunggren, S. *Langmuir* **1990**, *6*, 895.
- (43) Nagarajan, R.; Ruckenstein, E. *Langmuir* **1991**, *7*, 2934.
- (44) Jönsson, B.; Wennerström, H. *J. Phys. Chem.* **1987**, *91*, 338.
- (45) Gruen, D. W. R.; de Lacey, E. H. B. In *Surfactants in Solution*, Vol. 1; Mittal, K. L., Lindman, B., Eds.; Plenum Publishing Corp.: New York, 1984; p 279.
- (46) Strey, R.; Winkler, J.; Magid, L. *J. Phys. Chem.* **1991**, *95*, 7502.
- (47) Duns, G. J.; Reeves, L. W.; Yang, D. W.; Williams, D. S. *J. Colloid Interface Sci.* **1995**, *173*, 261.
- (48) Smith, G. A.; Christian, S. D.; Tucker, E. E.; Scamehorn, J. F. *J. Colloid Interface Sci.* **1989**, *130*, 254.
- (49) Faten, Z. M.; Higazy, W. S.; Christian, S. D.; Tucker, E. E.; Taha, A. A. *J. Colloid Interface Sci.* **1989**, *131*, 96.
- (50) McAuliffe, C. J. *J. Phys. Chem.* **1966**, *70*, 1267.
- (51) Boden, N.; Jones, S. A. In *Nuclear Magnetic Resonance of Liquid Crystals*; Emsley, J. W., Ed.; D. Reidel Publishing Co.: Dordrecht, 1985.
- (52) Landgren, M. Thesis, Lund, 1990.
- (53) Aamodt, M.; Landgren, M.; Jönsson, B. *J. Phys. Chem.* **1992**, *96*, 945.
- (54) Landgren, M.; Aamodt, M.; Jönsson, B. *J. Phys. Chem.* **1992**, *96*, 950.
- (55) Stilbs, P.; Walderhaug, H.; Lindman, B. *J. Phys. Chem.* **1983**, *87*, 4762.
- (56) Matheson, I. B. C.; King, A. D., Jr. *J. Colloid Interface Sci.* **1978**, *66*, 464.
- (57) Mely, B.; Charvolin, J.; Keller, P. *Chem. Phys. Lipids* **1975**, *15*, 161.
- (58) Walderhaug, H.; Söderman, O.; Stilbs, P. *J. Phys. Chem.* **1984**, *88*, 1655.
- (59) Néry, H.; Söderman, O.; Canet, D.; Walderhaug, H.; Lindman, B. *J. Phys. Chem.* **1986**, *90*, 5802.